EUKARYOTIC CELL, July 2006, p. 1091–1103 Vol. 5, No. 7
1535-9778/06/$08.00+0 doi:10.1128/EC.00139-06

Calcineurin Controls Growth, Morphology, and Pathogenicity in *Aspergillus fumigatus*

William J. Steinbach,[1,2]†* Robert A. Cramer, Jr.,[2]† B. Zachary Perfect,[1] Yohannes G. Asfaw,[3] Theodor C. Sauer,[1] Laura K. Najvar,[4] William R. Kirkpatrick,[4] Thomas F. Patterson,[4] Daniel K. Benjamin, Jr.,[1] Joseph Heitman,[2,5,6] and John R. Perfect[2,5]

Department of Pediatrics,[1] Department of Molecular Genetics and Microbiology,[2] Department of Laboratory Animal Resources,[3] Department of Medicine,[5] and Department of Pharmacology and Cancer Biology,[6] Duke University Medical Center, Research Drive, Durham, North Carolina 27710, and Department of Medicine, University of Texas Health Sciences Center at San Antonio, 7703 Floyd Curl Drive, MSC 7881, San Antonio, Texas 78229-3900[4]

Received 13 May 2006/Accepted 15 May 2006

Calcineurin is implicated in a myriad of human diseases as well as homeostasis and virulence in several major human pathogenic microorganisms. The fungus *Aspergillus fumigatus* is a leading cause of infectious death in the rapidly expanding immunocompromised patient population. Current antifungal treatments for invasive aspergillosis are often ineffective, and novel therapeutic approaches are urgently needed. We demonstrate that a mutant of *A. fumigatus* lacking the calcineurin A (*cnaA*) catalytic subunit exhibited defective hyphal morphology related to apical extension and polarized growth, which resulted in drastically decreased filamentation. The Δ*cnaA* mutant lacked the extensive lattice of invading hyphae seen with the wild-type and complemented strains. Sporulation was also affected in the Δ*cnaA* mutant, including morphological conidial defects with the absence of surface rodlets and the added presence of disjunctors creating long conidial chains. Infection with the Δ*cnaA* mutant in several distinct animal models with different types of immunosuppression and inoculum delivery led to a profound attenuation of pathogenicity compared to infection with the wild-type and complemented strains. Lung tissue from animals infected with the Δ*cnaA* mutant showed a complete absence of hyphae, in contrast to tissue from animals infected with the wild-type and complemented strains. Quantitative fungal burden and pulmonary infarct scoring confirmed these findings. Our results support the clinical observation that substantially decreasing fungal growth can prevent disease establishment and decrease mortality. Our findings reveal that calcineurin appears to play a globally conserved role in the virulence of several pathogenic fungi and yet plays specialized roles in each and can be an excellent target for therapeutic intervention.

The calcineurin pathway is an important signal transduction cascade required for T-cell activation and the target for the immunosuppressants cyclosporine A and FK506 (9, 19). Calcineurin is a highly conserved Ca^{2+}-calmodulin-activated protein phosphatase composed of a catalytic A subunit and a regulatory B subunit. Calcineurin is also a critical mediator of calcium signaling and numerous cell stress responses in eukaryotic organisms. Calcineurin regulation has been implicated in neuronal elongation (11), ion channel regulation (2), heart failure (32), Alzheimer's disease (18), and a myriad of other human conditions and cellular processes. Patients have been successfully treated with calcineurin inhibitors for a wide spectrum of diseases, most importantly to prevent and treat graft-versus-host disease (37), but also for other indications such as severe asthma (1), segmental glomerulosclerosis (28), refractory rheumatoid arthritis (38), atopic dermatitis, and others.

Fungi are an increasingly important cause of death among both immunocompetent (16) and immunocompromised (15) patients, and yet effective treatments are often lacking. Calcineurin is linked to several infectious agents, including human opportunistic pathogenic fungi such as *Cryptococcus neoformans* and *Candida albicans* (5, 24). Although calcineurin is highly conserved across higher and lower eukaryotes and even the fungal kingdom, it is utilized differently among the major pathogenic fungi. For instance, *Cryptococcus neoformans* mutants lacking calcineurin were severely growth impaired at 37°C (24), exhibited defects in hyphal elongation (10), and were avirulent (13). With *Candida albicans*, calcineurin was not required for in vitro survival at 37°C (5) but rather for survival in serum and virulence (3, 5, 33). It is clear based on these findings that one cannot always extrapolate from one fungal pathogen to another the function of a specific gene or network of genes, as unique ecological niches of individual fungi may result in novel functions for orthologous genes.

Invasive aspergillosis (IA) caused by the opportunistic pathogenic fungus *Aspergillus fumigatus* is a leading cause of infectious mortality in immunocompromised patients (21). While the mortality from invasive candidiasis caused by *Candida albicans* has decreased by 50% over the last two decades, the mortality associated with IA has increased 357% over the same period of time (22). Unfortunately, the optimal treatment for IA remains elusive. No study has examined the specific role of calcineurin in the pathogenicity of this increasingly

* Corresponding author. Mailing address: Division of Pediatric Infectious Diseases, Box 3499, Duke University Medical Center, Durham, NC 27710. Phone: (919) 681-1504. Fax: (919) 684-8902. E-mail: stein022@mc.duke.edu.

† W.J.S. and R.A.C. contributed equally to this work.

important fungal pathogen. Here we show that gene replacement of the calcineurin A (*cnaA*) locus with an auxotrophic selectable marker led to severe defects in the growth and development of the fungus. These defects substantially affected the ability of *A. fumigatus* to cause invasive disease, as multiple animal models of IA revealed the Δ*cnaA* mutant to be avirulent. Since calcineurin inhibition is successfully employed to treat human immune disorders, it may be possible to manipulate this pathway to develop novel treatment strategies for fungal infections such as the frequently fatal IA.

MATERIALS AND METHODS

Strains, media, and growth conditions. *Aspergillus fumigatus* strain AF293.1 was used to create the calcineurin A replacement (Δ*cnaA*) strain (Δ*cnaA*::*A. parasiticus pyrG*). AF293.1 is a uracil/uridine-auxotrophic (*pyrG*$^-$) mutant of *A. fumigatus* strain AF293 (25). AF293 was used as the wild-type strain for all animal model experiments. Preliminary animal model experiments showed no difference in virulence between AF293 and the *pyrG*-complemented AF293.1 strain. All *A. fumigatus* cultures were grown on glucose minimal media as previously described (34) at 37°C unless otherwise specified. An *Escherichia coli* One-Shot TOP10 strain (Invitrogen, Carlsbad, CA) was used for routine cloning and grown in Luria broth (Fisher Chemicals, Fair Lawn, NJ) supplemented with appropriate antibiotics at 37°C.

Creation of Δ*cnaA* mutant and Δ*cnaA* + *cnaA* complement in *A. fumigatus*. The 1.9-kb *A. fumigatus cnaA* gene (Afu5g09360; www.cadre.man.ac.uk) was replaced with the 3.1-kb *A. parasiticus pyrG* gene to create the Δ*cnaA* mutant (Fig. 1A). Approximately 1.1 kb of flanking sequence upstream and downstream of *cnaA* was cloned to flank the 3.1-kb *A. parasiticus pyrG* gene in plasmid pJW24 (a gift from Nancy Keller, University of Wisconsin—Madison) to create the replacement construct. *A. parasiticus pyrG* was used to complement the uracil auxotrophy of AF293.1. This resulting replacement construct plasmid was used as a template to create the ~5.3-kb PCR amplicon for use in transformation. AF293.1 (*pyrG*$^-$) was used as the recipient strain, and transformants were selected for growth in the absence of uracil/uridine supplementation. All primers used in this study are listed in Table 1.

Creation of fungal protoplasts and polyethylene glycol-mediated transformation of *A. fumigatus* were performed as previously described (7). Transformants were initially screened by PCR with primers designed to amplify the 1.9-kb *cnaA* gene, which should be absent in Δ*cnaA* strains. Transformants were additionally screened by PCR for the junctions of the *cnaA*::*pyrG* allele to indicate replacement and homologous recombination. Specifically, one flanking primer annealed to the *cnaA* locus outside the disruption construct and the second primer annealed within the *pyrG* sequence to create an amplicon in transformants that had undergone a homologous recombination event at the *cnaA* locus. Confirmation was performed via Southern analysis using a digoxigenin labeling system (Roche Molecular Biochemicals, Mannheim, Germany) and a 1.1-kb probe of the 5′ *cnaA* flanking sequence as well as a probe for the *A. parasiticus pyrG* gene.

The Δ*cnaA* mutant was complemented by transformation with the wild-type *cnaA* gene and 1 kb of flanking upstream and downstream sequence. An ~4.0-kb complementation construct PCR product was then transformed as detailed above into the recipient Δ*cnaA* mutant. No selectable markers were used, and transformants were selected by phenotypic restoration of filamentation. PCR and Southern analyses were performed as described above to confirm that isolates contained both the original *cnaA*::*pyrG* deletion allele and a single ectopic copy of the wild-type *cnaA* gene (Δ*cnaA* + *cnaA* strain).

Radial growth, mycelial mass, and conidiation. Radial growth on solid media was obtained by measuring colony diameters of the wild-type, Δ*cnaA* mutant, and Δ*cnaA* + *cnaA* strains once every 24 h over a period of 96 h. The inoculum was 10 to 1,000 conidia (1 μl of 1×10^4 to 1×10^6 conidia/ml) inoculated on glucose minimal medium agar and grown at 37°C. Each inoculum of each strain was done in triplicate, and the mean and standard error of colony diameter at each 24-h period are reported. Growth analysis in liquid culture was performed in triplicate using an inoculum of 1×10^6 conidia/ml in glucose minimal medium broth and incubated with shaking at 37°C. Growth was analyzed at 24, 48, 72, and 144 h and 14 days of growth. Mycelial mass in liquid culture was quantified in triplicate using 1×10^6 conidia/ml in glucose minimal medium broth incubated at 37°C for the stated durations, lyophilized overnight, and weighed.

Conidiation was quantified by harvesting conidia from the wild-type, Δ*cnaA* mutant, and Δ*cnaA* + *cnaA* strains. Strains were inoculated as 10 μl of 1×10^6 conidia/ml onto glucose minimal medium agar and incubated for 96 h. Incubation occurred at four different temperatures (25°C, 30°C, 37°C, and 40°C) to assay any effect on temperature and conidiation. Conidia were harvested with 10 ml of sterile 0.05% Tween 80, filtered through miracloth (EMD Biosciences, La Jolla, CA), and quantified with a hemacytometer. Harvests from each strain at each temperature were performed in triplicate, and the mean and standard error of the total number of conidia per ml collected from each strain at each temperature are reported.

Light and scanning electron microscopy. All light microscopy was performed with a Zeiss microscope using Nomarski optics (differential interference contrast). The wild-type, Δ*cnaA* mutant, and Δ*cnaA* + *cnaA* strains were grown at 1×10^6 conidia/ml in glucose minimal medium broth and fixed after sampling in 10% neutral buffered formalin. All scanning electron microscopy images were obtained by using an environmental scanning electron microscope (Philips XL30 ESEM TMP; FEI Company, Hillsboro, OR). For hyphal examination, starting cultures of 1×10^6 conidia/ml were grown in glucose minimal medium broth for 18 h at 37°C, washed twice in sterile water, and then air dried before viewing. For conidium examination, starting cultures of 20 μl of 1×10^6 conidia/ml were grown on glucose minimal medium agar plates for 48 h at 37°C and the conidia were harvested from a fresh plate with double-sided tape. Conidia were treated with a sputter coater (Hummer 6.2; Anatech, Springfield, VA) prior to examination.

Murine inhalational model of invasive aspergillosis. Six-week-old CD1 male mice (Charles River Laboratories) (mean weight, 22.5 g) were immunosuppressed with both cyclophosphamide (Cytoxan; Bristol-Myers Squibb, Princeton, NJ) at 150 mg/kg of body weight administered intraperitoneally (i.p.) on days −2 and +3 of infection and triamcinolone acetonide (Kenalog-40; Bristol-Myers Squibb, Princeton, NJ) at 40 mg/kg administered subcutaneously (s.c.) on days −1 and +6 of infection. Mice were housed under sterile conditions and supplied sterile drinking water supplemented with vancomycin (1 mg/ml), gentamicin (0.2 mg/ml), and clindamycin (1 mg/ml). Four groups of 20 immunosuppressed, unanesthetized mice each inhaled 40 ml of an aerosolized suspension of 1×10^9 conidia/ml of the wild-type, Δ*cnaA* mutant, or Δ*cnaA* + *cnaA* strain or diluent control (0.05% Tween 80) in a Hinners inhalational chamber for 30 min as previously described (35). Mice were evaluated for morbidity and mortality in a blinded fashion twice daily. Survival was plotted on a Kaplan-Meier curve for each *Aspergillus* strain, and a log rank test was used for pairwise comparison of survival. Statistical significance was defined as a two-tailed P value of <0.05.

Other distinct animal models of invasive aspergillosis. Studies with a separate murine inhalational model conducted at a second laboratory used outbred ICR mice (Harlan Sprague Dawley, Indianapolis, IN) (weight range, 19 to 21 g) immunosuppressed with cyclophosphamide at 250 mg/kg administered i.p. and cortisone acetate at 250 mg/kg administered s.c. 2 days prior to infection and then again on the third day after infection with cyclophosphamide at 200 mg/kg administered i.p. and cortisone acetate at 250 mg/kg administered s.c. Mice were administered ceftazidime at 50 mg/kg s.c. daily to prevent bacterial infection. Four groups of 20 immunosuppressed mice inhaled an aerosolized suspension of 1×10^9 conidia/ml of the wild-type, Δ*cnaA* mutant, or Δ*cnaA* + *cnaA* strain or diluent control for 1 h in an acrylic aerosol chamber. Mice were evaluated in a fashion similar to that for the other inhalational model system.

The wild-type, Δ*cnaA* mutant, and Δ*cnaA* + *cnaA* strains or diluent control were all used in additional separate animal models of invasive aspergillosis. In a murine intranasal model, 8-week-old DBA/2 male mice (Jackson Laboratories, Bar Harbor, ME) (mean weight, 22 g) were immunosuppressed with a single dose of triamcinolone acetonide at 40 mg/kg 1 day prior to infection. Four groups of 10 immunosuppressed mice were intranasally infected with 3×10^4 conidia (30 μl of 1×10^6 conidia/ml). In a murine intravenous model, 6-week-old CD1 male mice (mean weight, 22 g) were not immunosuppressed and four groups of 10 mice were intravenously infected through the lateral tail vein with 8×10^6 conidia (200 μl of 4×10^7 conidia/ml) as previously described (8). In an invertebrate model, sixth-instar larvae of the greater wax moth, *Galleria mellonella* (Vanderhorst Inc., Saint Marys, OH) (17, 31), were infected into the hemocoel with 1×10^6 conidia (5 μl of 2×10^8 conidia/ml) as previously described (23). Four groups of 15 larvae were infected. Survival was plotted on a Kaplan-Meier curve for all animal models, and a log rank test was used for pairwise comparison of survival. Statistical significance was defined as a two-tailed P value of <0.05. The IACUC committees of both Duke University and the University of Texas Health Science Center at San Antonio approved all respective murine protocols.

Histopathologic and CFU quantification of fungal burden. To evaluate in vivo histopathologic progression of disease, four groups of nine additional mice were similarly infected in the first murine inhalational model with each strain and euthanized at defined time points (days +3, +5, and +7 after infection). Lungs were harvested and stained with hematoxylin and eosin to characterize inflam-

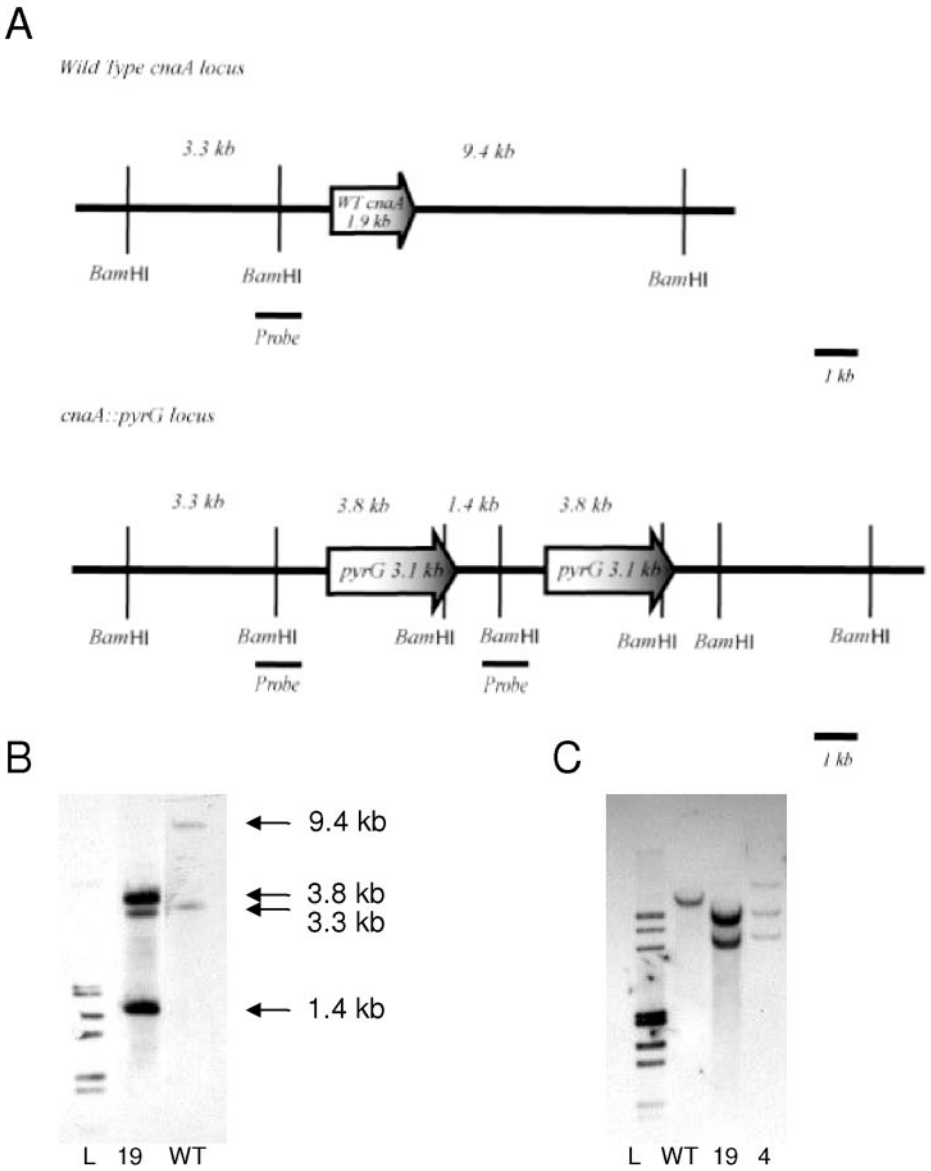

FIG. 1. Construction of Δ*cnaA* mutant and complement of *A. fumigatus*. (A) In the Δ*cnaA* mutant, wild-type *A. fumigatus cnaA* (1.9 kb) is replaced by the 3.1-kb *A. parasiticus pyrG* gene. The Δ*cnaA* mutant was created by tandem insertional replacement of the *pyrG* in the *cnaA* locus. The short, dark bar is the 1.1-kb probe of the upstream flanking sequence used for Southern analyses. (B) Southern analyses were performed on BamHI-digested genomic DNA which was probed with the 1.1-kb probe of the upstream flanking sequence to demonstrate a tandem insertion and replacement of *cnaA*. Additional Southern analyses with HindIII-, KpnI-, ApaI-, and NdeI-digested genomic DNA and probing with both the upstream flanking sequence and a *pyrG* probe (data not shown) confirmed the tandem insertion. (C) Complementation of the Δ*cnaA* mutant was confirmed by AgeI-digested genomic DNA probed with the same 1.1-kb probe to reveal both the *cnaA*::*pyrG* deletion allele and a single ectopic copy of the wild-type *cnaA* gene (Δ*cnaA* + *cnaA* strain). L, ladder; WT, wild type; 19, Δ*cnaA* mutant; 4, Δ*cnaA* + *cnaA* strain.

mation and Gomori's methenamine silver stain to document fungal invasion. A veterinary murine pathologist evaluated each lung section in a blinded fashion to quantify infection according to a five-point pulmonary infarct score that incorporated necrosis, hemorrhage, edema, and hyphal presence as previously described (35).

In order to quantify fungal burden of disease, four groups of 30 additional mice were similarly infected in the second laboratory's murine inhalational model and euthanized at defined time points (days +3, +5, and +7 after infection) for determination of CFU in the lungs. Additionally, five mice infected with each strain were evaluated for CFU in the lung at 1 h after infection to document uniform exposure with each strain. The Kruskal-Wallis test with Dunn's posttest was used for analysis of fungal burden.

RESULTS

***A. fumigatus* strain creation.** To study the role of calcineurin in *A. fumigatus* tissue invasion and pathogenicity, we successfully constructed a calcineurin A-deficient mutant by replacing the *A. fumigatus cnaA* gene with the *A. parasiticus pyrG* gene (Fig. 1A). Transformation of the uracil/uridine-auxotrophic *A. fumigatus* strain AF293.1 with the *cnaA* replacement construct yielded 28 transformants, including 9 with a profound lack of filamentation and growth on glucose minimal medium agar.

TABLE 1. Primers used in this study

Primer	Sequence (5′ to 3′)	Function
cnaApyrGcloneFor	TAGTCGACAAGGGGACTTGG	Clone 5′ *cnaA* flank
cnaApyrGcloneRev	TAGAATTCCTTGCGCAGTGTG	Clone 5′ *cnaA* flank
cnaApyrGcloneFor	ATGCGGCCGCAATTGCTTCGGTCACGTCCATG	Clone 3′ *cnaA* flank
cnaApyrGcloneRev	ATGAGCTCGCGGTCGCGTCATTTAAACC	Clone 3′ *cnaA* flank
cnaAKOcolonyup	GTATAGGGAAGAGTAACCGAGGTC	Outside 5′ flank construct
pyrGseqrightjxn	TGGGCCTAGAATATTCCATCAG	Inside *pyrG* 5′ flank
pyrGseqleftjxn	TAGCGCTATATGCGTTGATGC	Inside *pyrG* 3′ flank
cnaAKORT	GGCTTAATACCGGATCAGCAAGC	Outside 3′ flank construct
cnaACadreStartPstI	ATATCTGCAGATGGATCAAGCACTGGCGCGC	Wild-type *cnaA* 5′
cnaACadreRevPstI	ATATCTGCAGTTAGGCTTCCCTAGTCTCCCG	Wild-type *cnaA* 3′
cnaApyrGcomplSpeI	CTAGACTAGTTTGCCTATTTCACATCCAACC	*cnaA* complement 5′
cnaApyrGcomplPstI	CTAGCTGCAGACAAAACCACAGTCTTTTTAG	*cnaA* complement 3′
Realtime-cnaAFor	CATCGGACGTCTCTCGCGTGTC	Real-time *cnaA* 5′
Realtime-cnaARev	GCGCCAAGCATCAGGGTACCAG	Real-time *cnaA* 3′
Realtime-actinFor	TCACTGCCCTTGCTCCCTCGTC	Real-time actin 5′
Realtime-actinRev	GCACTTGCGGTGAACGATCGAA	Real-time actin 3′

Eight transformants were further analyzed, four with filamentation defects and four with no obvious filamentation defect. The four transformants with filamentation defects had both PCR amplicons with primers designed to amplify the predicted *cnaA* replacement locus after homologous recombination and no detectable PCR amplicon with primers designed to amplify the wild-type *cnaA* locus. The four transformants without any obvious filamentation defects each lacked PCR amplicons for the replacement locus and had amplicons for the wild-type locus.

To confirm *cnaA* replacement, Southern analysis with BamHI-digested genomic DNA was performed (Fig. 1B). Wild-type strain AF293 yielded predicted bands of 3.3 kb and 9.4 kb, while in the four transformants (CNAKO-7, -16, -18, and -19) with filamentation defects there were bands of 3.3 kb, 3.8 kb, and 1.4 kb and absence of the 9.4-kb band. This confirmed the predicted replacement of *cnaA* with *pyrG* and the 1.4-kb band via a tandem insertion of the replacement construct into the *cnaA* locus. Two of the mutants had banding patterns that suggested multiple insertions of the replacement construct (CNAKO-16 and -18), so those transformants were not further pursued. The remaining two mutants underwent repeat Southern analysis with HindIII-, KpnI-, ApaI-, and NdeI-digested genomic DNA, and all yielded predicted band sizes consistent with a tandem insertion of the replacement construct into the *cnaA* locus. Additional Southern analysis using a probe for the 3.1-kb *A. parasiticus pyrG* gene yielded a single band in both mutants and an absence of a band in the wild type, suggesting a single insertion of the replacement allele into the *cnaA* locus. One of the two mutants, CNAKO-19, was then chosen and single spore isolated twice. Southern analyses were repeated after single spore isolation to confirm the replacement, and this strain was renamed the Δ*cnaA* mutant for continuation throughout the in vitro and animal model experiments. The other mutant, CNAKO-7, underwent in vitro growth and conidiation experiments and yielded results similar to those for CNAKO-19 but was not continued for the extensive animal model experiments.

To complement the *cnaA* defect in the Δ*cnaA* mutant strain, a PCR product containing the entire *cnaA* wild-type locus plus 1 kb of additional 5′ and 3′ sequence was transformed into the recipient Δ*cnaA* mutant strain and colonies were selected based on restoration of filamentation. A total of seven transformants with normal filamentation and growth were obtained. PCR screening of three transformants (CNACOMP-2, -4, and -6) with the same primers as for the replacement yielded all three strains with the flanking products, indicating preservation of the *cnaA*::*pyrG* replacement locus as well as restoration of *cnaA* and thus an ectopic insertion of the *cnaA* complementation construct. Southern analysis with AgeI-digested genomic DNA revealed that all three transformants had ectopic insertions of the *cnaA* complementation construct, but only one (CNACOMP-4) had a single insertion event (Fig. 1C). CNACOMP-4 was single spore isolated twice, and Southern analyses were repeated to confirm the complementation. This strain was renamed the Δ*cnaA* + *cnaA* strain for continuation throughout the in vitro and animal model experiments. Confirmation of *cnaA* gene replacement and complementation was also assessed using real-time reverse transcriptase PCR to amplify a 117-bp section of *cnaA*. PCR results revealed gene expression of *cnaA* in both the wild-type and Δ*cnaA* + *cnaA* strains but not the Δ*cnaA* mutant.

Calcineurin is necessary for filamentous growth. The Δ*cnaA* mutant had profound defects in filamentation and growth compared to the wild-type and Δ*cnaA* + *cnaA* strains (Fig. 2A). After 21 days of growth on glucose minimal medium agar, Δ*cnaA* mutant colonies grew only 3 cm, whereas wild-type and Δ*cnaA* + *cnaA* colonies grew rapidly and completely filled the agar surface with expanding filaments. Quantification of radial growth (Table 2) confirmed the dramatically stunted growth of the Δ*cnaA* mutant compared to that of the wild-type and Δ*cnaA* + *cnaA* strains. The Δ*cnaA* mutant phenotype was apparent regardless of inoculum concentration; all concentrations (1×10^2 to 1×10^6 conidia) demonstrated a severely restricted growth pattern with a lack of appreciable lateral filamentation and limited aerial growth. The growth and filamentation defects in the Δ*cnaA* mutant compared to the wild-

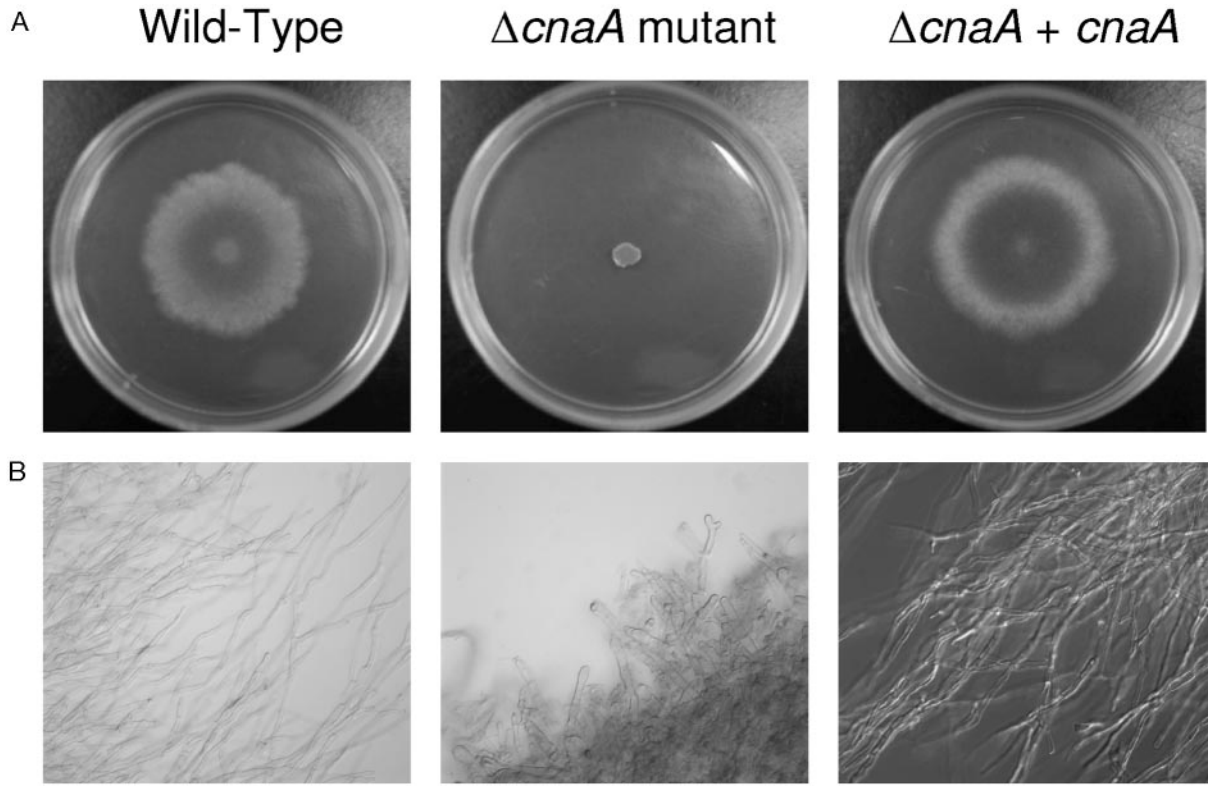

FIG. 2. Calcineurin is necessary for filamentous growth. (A) *A. fumigatus* conidia (1×10^3 conidia/ml) were incubated on glucose minimal media at 37°C for 96 h, revealing poor growth and filamentation in the Δ*cnaA* mutant. (B) *A. fumigatus* conidia (1×10^6 conidia/ml) grown in glucose minimal medium broth at 37°C were sampled at specified time points (144 h is shown), demonstrating blunted hyphal growth of the Δ*cnaA* mutant. Magnification, ×40 with Nomarski optics (differential interference contrast). Bar, 5 μm.

type and Δ*cnaA* + *cnaA* strains were also unaffected by incubation at several temperatures (25°C, 30°C, 37°C, and 40°C).

In liquid culture, Δ*cnaA* mutant hyphae appeared more compact, more dense, and extremely blunted, while the hyphae of the wild-type and Δ*cnaA* + *cnaA* strains formed long, branching, dispersed filaments (Fig. 2B) that were indistinguishable from each other. Analyses at 24, 48, 72, and 144 h and later at 14 days of growth all demonstrated no significant advancement in hyphal extension in the Δ*cnaA* mutant. Mycelial dry weight of the Δ*cnaA* mutant was also decreased compared to that of the wild-type and Δ*cnaA* + *cnaA* strains (Table 3). There were no in vitro growth conditions found in which the Δ*cnaA* mutant exhibited near-wild-type growth. However, dark-field microscopy revealed the presence of septa in the Δ*cnaA* mutant.

Examination by scanning electron microscopy revealed pro-

TABLE 2. Severely restricted radial growth of *A. fumigatus* Δ*cnaA* mutant

A. fumigatus strain	Starting inoculum (no. of conidia)	Radial growth (mm [mean ± SE]) at:			
		24 h	48 h	72 h	96 h
Wild type	10	0 ± 0	12.3 ± 0.33	24.7 ± 0.33	36.0 ± 0.10
	100	0 ± 0	14.7 ± 0.33	26.0 ± 0.10	38.0 ± 0.10
	1,000	3.0 ± 0.33	18.0 ± 0.10	29.3 ± 0.33	43.0 ± 0.33
Δ*cnaA* mutant	10	0 ± 0	1.0 ± 0.10	1.7 ± 0.33	2.7 ± 0.33[a]
	100	0 ± 0	3.0 ± 0.10	4.0 ± 0.10	4.0 ± 0.10[b]
	1,000	3.0 ± 0.33	4.0 ± 0.10	4.0 ± 0.10	4.7 ± 0.33[c]
Δ*cnaA* + *cnaA*	10	0 ± 0	13.0 ± 0.33	26.0 ± 0.58	39.0 ± 0.10[d]
	100	0 ± 0	15.7 ± 0.33	28.0 ± 0.58	40.7 ± 0.33[d]
	1,000	3.0 ± 0.33	19.3 ± 0.33	32.3 ± 0.33	44.0 ± 0.58[d]

[a] $P = 0.03$ versus result for the corresponding inoculum of the wild type.
[b] $P = 0.02$ versus result for the corresponding inoculum of the wild type.
[c] $P = 0.04$ versus result for the corresponding inoculum of the wild type.
[d] $P = 0.57$ versus result for the corresponding inoculum of the wild type.

TABLE 3. Decreased mycelial mass of *A. fumigatus* Δ*cnaA* mutant

A. fumigatus strain	Mycelial mass (g [mean ± SE]) at:			
	24 h	48 h	72 h	96 h
Wild type	0.550 ± 0.03	1.189 ± 0.07	3.764 ± 0.08	4.103 ± 0.08
Δ*cnaA* mutant	0.249 ± 0.03	0.689 ± 0.05	1.158 ± 0.06	1.467 ± 0.04[a]
Δ*cnaA* + *cnaA*	0.537 ± 0.01	1.379 ± 0.07	3.896 ± 0.09	4.161 ± 0.04

[a] $P = 0.049$ versus result for the wild type.

found hyphal loss and blunting in the Δ*cnaA* mutant compared to the wild-type and Δ*cnaA* + *cnaA* strains (Fig. 3). The resulting dense mass of shortened hyphae lacked the extensive lattice of invading hyphae seen with the wild-type and complemented strains. There were no clear hyphal extensions seen, as many of the hyphal arms were absent at the point of branching, creating a distinct "club" appearance. These results all suggest that calcineurin is required for normal filamentous growth in *A. fumigatus*.

Calcineurin is necessary for normal conidiation. In addition to defects in filamentation and growth, the *A. fumigatus* Δ*cnaA* mutant was found to have substantial conidiation defects. To understand the effect of environmental influences on conidiation of the Δ*cnaA* mutant, we examined several different conditions. Quantitative conidiation assays demonstrated a significant decrease in conidium production at each of several temperatures (25°C, 30°C, 37°C, and 40°C) in the Δ*cnaA* mutant compared to levels for the wild-type and Δ*cnaA* + *cnaA* strains. For example, mean conidia harvested after growth at 37°C for the wild-type, Δ*cnaA* mutant, and Δ*cnaA* + *cnaA* strains were 1.12×10^8, 9.15×10^6, and 1.55×10^8 conidia per ml, respectively. Conidiation by the Δ*cnaA* mutant was also markedly inhibited at extreme pHs, 4.5 and 9.5, compared to that of the other strains but was similar to that of the wild-type and Δ*cnaA* + *cnaA* strains at pH 5.5 to 7.5, suggesting a decreased ability to produce conidia under more stressful environmental conditions. All other experiments utilized glucose minimal media with a standard pH of 6.5 (34).

Higher magnification with scanning electron microscopy revealed two prominent morphological conidial defects in the Δ*cnaA* mutant that were not apparent by observation on solid media. The conidia of wild-type *A. fumigatus* are coated with hydrophobic proteins called rodlets which extend out from the conidial surface and are thought to be related to conidial adhesive properties (39). However, the Δ*cnaA* mutant conidia appeared to lack these surface rodlets (Fig. 4) and instead to possess smooth conidial surfaces. Also, the Δ*cnaA* mutant conidia did not appear as single, dispersed conidia, as did conidia of the wild-type and Δ*cnaA* + *cnaA* strains, but rather only as long chains of conidia that required 0.05% Tween 80 for separation. The Δ*cnaA* mutant conidia were connected via disjunctors, generally thought to be cellular junctions between conidia, which linked the normally individual conidia.

Calcineurin is required for pathogenicity in distinct animal models. To test the virulence of the Δ*cnaA* mutant, a murine inhalational model of invasive pulmonary aspergillosis was utilized to mimic human disease (35). Infection with the wild-type strain yielded 90% mortality by 14 days after infection (Fig. 5A), while infection with the Δ*cnaA* mutant led to only 10% mortality ($P < 0.001$). The remaining animals infected with the wild-type strain died 17 days after infection, while all animals infected with the Δ*cnaA* mutant survived until the experiment was terminated at 28 days. Importantly, animals infected with the Δ*cnaA* mutant were symptomatically indistinguishable from uninfected control animals during the entire experimental course. Animals infected with wild-type and Δ*cnaA* + *cnaA* strains displayed progressive and severe signs of invasive disease that have been well described previously, including ruffled fur, hunched posture, and an increased respiratory rate. A likely explanation for the restoration of in vitro growth and conidiation and yet an incomplete restoration of pathogenicity of the Δ*cnaA* + *cnaA* strain in the animal model is the inoculum utilized. Each strain was diluted to approximately 1×10^9 conidia/ml prior to infection, but quantification just after inoculum delivery revealed a markedly lower inoculum in the Δ*cnaA* + *cnaA* strain (2.3×10^7 conidia/ml) than in the wild type (6.8×10^8 conidia/ml) and the Δ*cnaA* mutant (1.3×10^9 conidia/ml). This corresponds to our preliminary work where a lower infectious inoculum led to decreased mortality (35).

Additional fundamentally distinct animal models, all with purposefully unique attributes encompassing animal species, immunosuppression, inoculum, and delivery, were employed to robustly demonstrate the lack of pathogenicity with the Δ*cnaA* mutant. Intranasal, intravenous, and additional inhalational murine models as well as an invertebrate wax moth larva model all demonstrated similar profound attenuations of pathogenicity following infection with the Δ*cnaA* mutant compared to results following infection with the wild-type and Δ*cnaA* + *cnaA* strains (Fig. 6).

Another model of murine inhalational invasive pulmonary aspergillosis was performed in a second laboratory with a different immunosuppressive regimen and a different animal strain. This ensured that results of Δ*cnaA* mutant disease would not be laboratory or host specific through changing the technical and host factors. This second inhalational model demonstrated that infection with the wild-type strain yielded 100% mortality by 11 days after infection, while infection with the Δ*cnaA* mutant led to only 5% mortality ($P < 0.001$). In the murine intranasal model of invasive pulmonary aspergillosis, infection with the wild-type strain yielded 50% mortality by 14 days after infection, while infection with the Δ*cnaA* mutant led to 0% mortality ($P = 0.011$). In the murine intravenous model of invasive systemic aspergillosis, infection with the wild-type strain yielded 50% mortality by 14 days after infection, while infection with the Δ*cnaA* mutant again led to 0% mortality ($P = 0.012$). The invertebrate wax moth model of invasive aspergillosis showed findings similar to those of the murine models. Specifically, infection with the wild-type strain yielded 80% mortality by 5 days after infection, while infection with the Δ*cnaA* mutant led to 7% mortality ($P < 0.001$). In every animal model, inoculation with the diluent control (0.05% Tween 80) resulted in 0% mortality.

Infection with the Δ*cnaA* mutant results in decreased invasion and fungal burden. Histopathologic analysis revealed extensive invasive hyphae throughout lung sections from additional animals infected in the murine inhalational model with both the wild-type and Δ*cnaA* + *cnaA* strains but a complete absence of hyphae in animals infected with the Δ*cnaA* mutant at all time points examined (Fig. 5B). Additionally, there was minimal lung inflammation in animals infected with the Δ*cnaA*

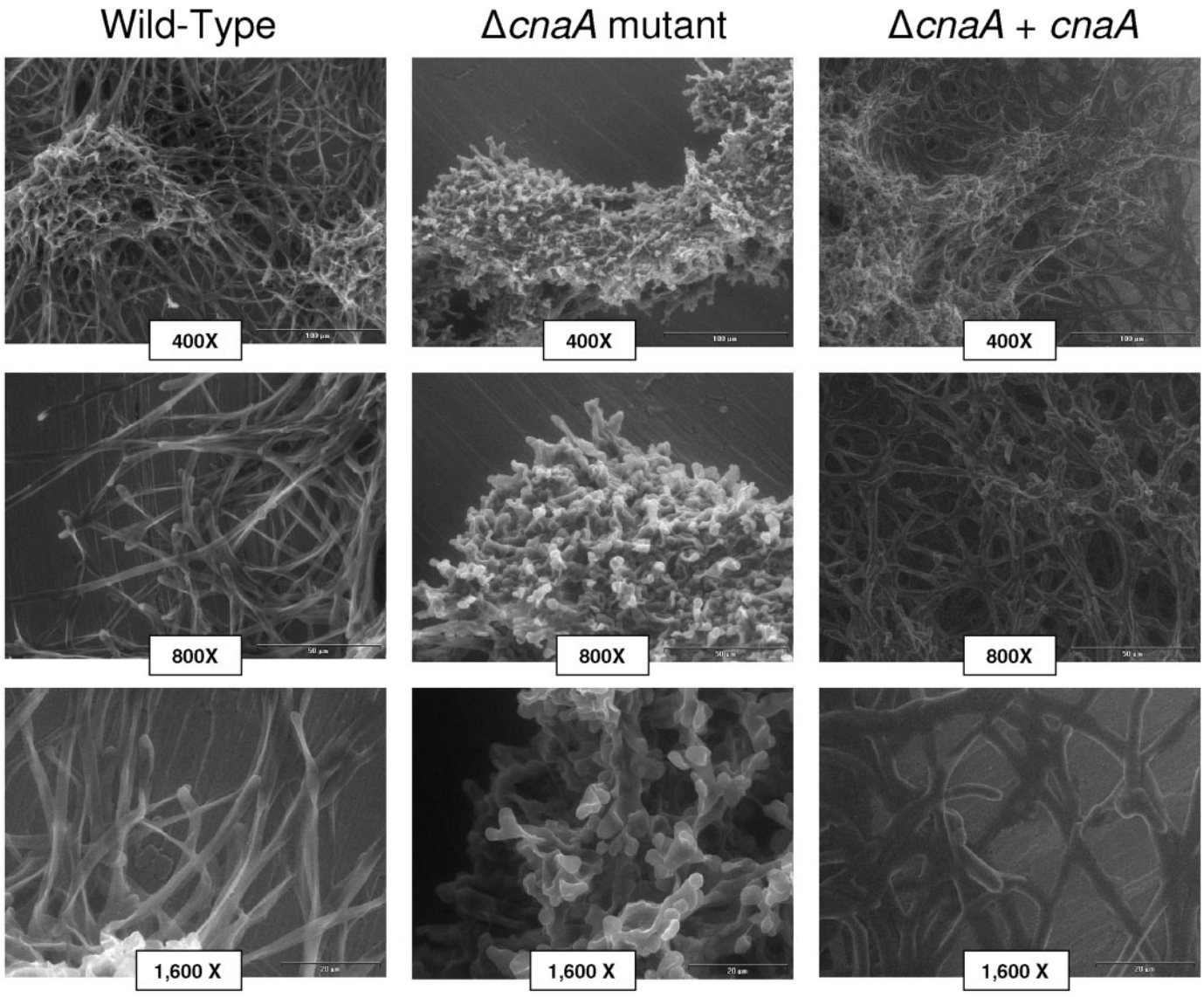

FIG. 3. Calcineurin mutant creates dense, extremely blunted hyphae. *A. fumigatus* conidia (1×10^6 conidia/ml) were grown in glucose minimal medium broth for 18 h at 37°C. Δ*cnaA* mutant hyphae show profound blunting that leads to a more compact hyphal mass, while the wild-type and Δ*cnaA* + *cnaA* strains show similar normal morphologies. Levels of magnification by environmental scanning electron microscopy are shown. Bars, 100 μm (top row), 50 μm (middle row), and 20 μm (bottom row).

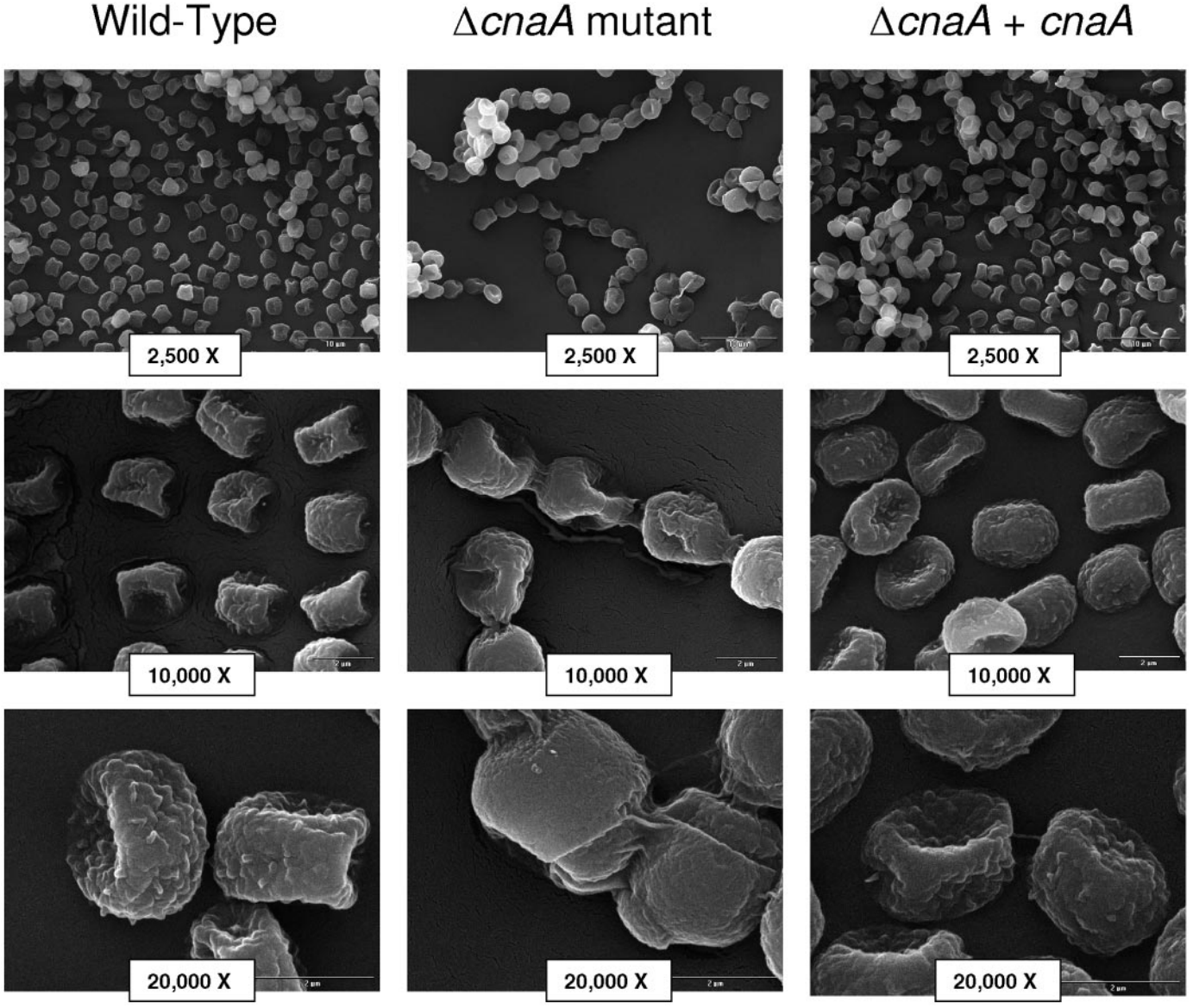

FIG. 4. Calcineurin is necessary for normal conidiation. Cultures of 20 μl of 1×10^6 conidia/ml were grown on glucose minimal medium agar for 48 h at 37°C. Conidia of the Δ*cnaA* mutant showed clumping and disjunctors formed between individual conidia as well as the absence of rodlets. Levels of magnification by environmental scanning electron microscopy are shown. Bars, 10 μm (top row) and 2 μm (middle and bottom rows).

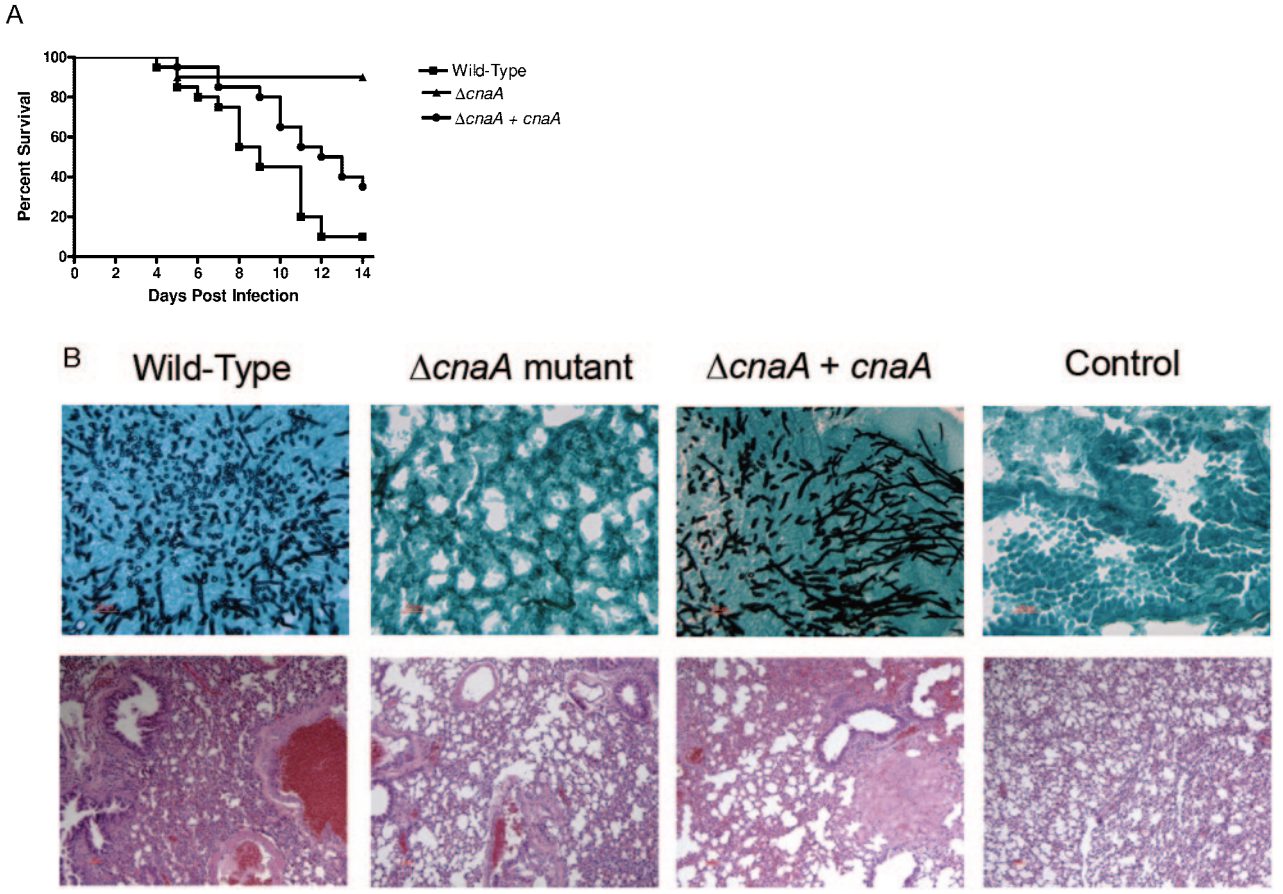

FIG. 5. Calcineurin is essential for pathogenicity and tissue invasion. (A) Kaplan-Meier survival curve of murine inhalational model of invasive pulmonary aspergillosis demonstrates that infection with the wild-type strain results in 90% mortality, while infection with the Δ*cnaA* mutant results in only 10% mortality ($P < 0.001$). Each experimental arm consisted of 20 mice. (B) Lung histopathologic examination at 7 days after infection in the murine inhalational model. (Top row) Gomori's methenamine silver staining showed no hyphae in the animals infected with the Δ*cnaA* mutant but substantial hyphal tissue invasion in the animals infected with the wild-type and Δ*cnaA* + *cnaA* strains. Magnification, ×40. (Bottom row) Hematoxylin and eosin staining showed only minimal inflammation in the animals infected with the Δ*cnaA* mutant but consistent inflammation and alveolar destruction in the animals infected with the wild-type and Δ*cnaA* + *cnaA* strains. Magnification, ×10.

mutant and a greater number of normal, open alveoli. In animals infected with wild-type and Δ*cnaA* + *cnaA* strains, infiltration of the alveoli with phagocytic cells and debris and alveolar destruction were observed. Uninfected control mice showed no architectural changes in the lungs.

Pulmonary infarct scores (35) at each time point during infection were greater for the wild-type and Δ*cnaA* + *cnaA* strains than for the Δ*cnaA* mutant. The mean pulmonary infarct score at 7 days after infection for the Δ*cnaA* mutant was 0, compared to a mean score of 8.5 for the wild-type strain and 9.0 for the Δ*cnaA* + *cnaA* strain. The only pulmonary damage seen with the Δ*cnaA* mutant at any time point occurred after 7 days of infection and involved only slight inflammation but no apparent hyphae, necrosis, hemorrhage, or edema in the lung tissue. In the immunosuppressed, uninfected control mice, there were no findings of necrosis, hemorrhage, or edema at any time point.

In the separate evaluation of quantitative fungal burden in the murine inhalational model, infection with the Δ*cnaA* mutant demonstrated significantly less lung fungal burden at all three time points examined than did infection with the wild-type or Δ*cnaA* + *cnaA* strain (Table 4). This third measure again demonstrated the lack of in vivo growth, lung invasion, and disease establishment with the Δ*cnaA* mutant. The absence of rodlets and conidial clumping in the Δ*cnaA* mutant originally suggested a possible mechanistic barrier to descending into the alveoli to explain the lack of virulence and decreased fungal burden in the inhalational model. However, analysis of animal lungs 1 h after inhalation revealed the clear presence of CFU from the Δ*cnaA* mutant, wild-type, and Δ*cnaA* + *cnaA* strains (3.53 ± 0.16, 4.46 ± 0.24, and 4.34 ± 0.21 $\log_{10}$ CFU/g lung tissue [means ± standard errors], respectively). Although there was significant reduction in the fungal burden reaching the lungs ($P = 0.0092$), likely due to the Δ*cnaA* mutant's conidial defect, this confirmed that the virulence defect was not due simply to a complete lack of inhalation of the Δ*cnaA* mutant but also to the mutant's inability to grow and produce disease directly within the tissue.

DISCUSSION

In this study, we report the creation of an *A. fumigatus* strain deficient in calcineurin A. The *cnaA* gene in *A. fumigatus* is not

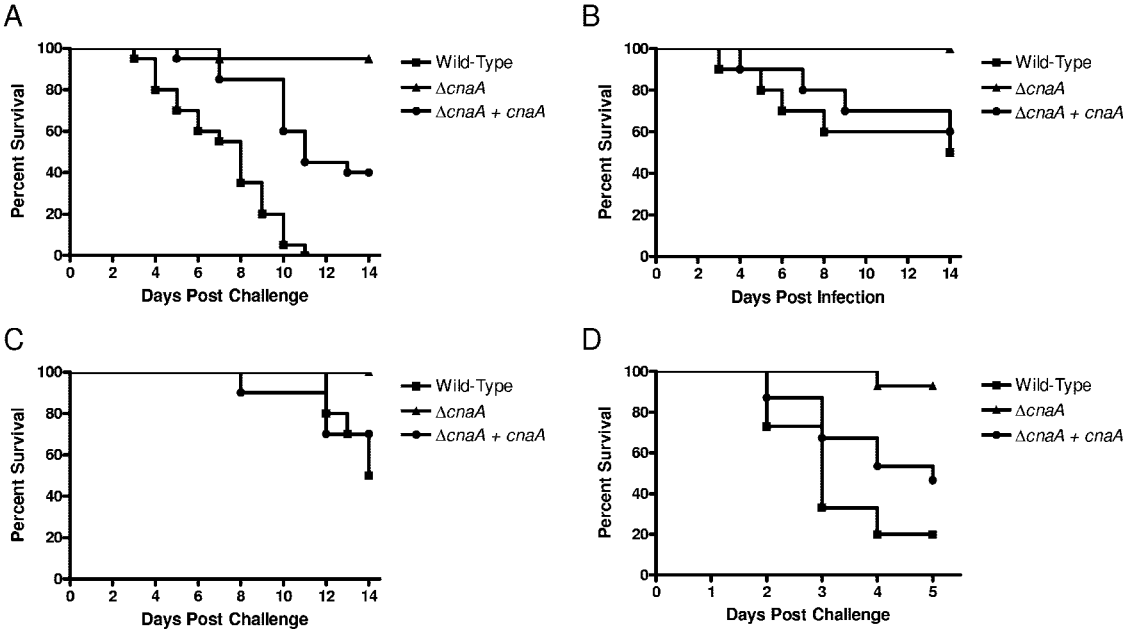

FIG. 6. Calcineurin is essential for pathogenicity in additional animal models. (A) The second laboratory's murine inhalational model demonstrated 100% mortality for animals infected with the wild-type strain, compared to only 5% mortality for animals infected with the Δ*cnaA* mutant ($P < 0.001$). Each experimental arm consisted of 20 mice. (B) Infection via intranasal delivery with the wild-type strain yielded 50% mortality, compared to 0% mortality for animals infected with the Δ*cnaA* mutant ($P = 0.011$). Each experimental arm consisted of 10 mice. (C) Infection via intravenous delivery with the wild-type strain yielded 50% mortality, compared to 0% mortality for animals infected with the Δ*cnaA* mutant ($P = 0.012$). Each experimental arm consisted of 10 mice. (D) Infection of the wax moth larvae with the wild-type strain yielded 80% mortality, compared to only 7% mortality for larvae infected with the Δ*cnaA* mutant ($P < 0.001$). Each experimental arm consisted of 15 larvae.

an essential gene, in contrast to *cnaA* in the related species *A. nidulans* (30), which is now understood to be distantly related based on recent whole-genome analyses (14). The *A. fumigatus* Δ*cnaA* mutant displays significant physiological defects that critically affect the fitness of the fungus. While not lethal, replacement of the *cnaA* gene leads to extremely stunted growth in *A. fumigatus*, suggesting that calcineurin plays a global regulatory role in morphology, growth, and conidial formation.

The drastic in vitro phenotypic defects associated with fungal growth seen with the Δ*cnaA* mutant likely led to a significant decrease in its ability to establish disease even in an immunocompromised host. The conidia are the infectious propagules that initiate human disease upon inhalation of this ubiquitous fungus. The Δ*cnaA* mutant formed unique long conidial chains, and electron microscopy showed the conidia of the Δ*cnaA* mutant linked by disjunctors. Surface rodlets, formed by hydrophobins, appeared to be absent on the Δ*cnaA* mutant. A deletion of a gene for rodlet formation (Δ*rodA*) in *A. fumigatus* had no effect on virulence (39), so it is unlikely that the absence of rodlets alone contributed to the significant pathogenicity defect seen with the Δ*cnaA* mutant. An association between *rodA* and the calcineurin pathway and molds has not previously been established, and expression of *rodA* was not examined with the Δ*cnaA* mutant. Thus, it is not clear if *cnaA* directly regulates rodlet formation.

TABLE 4. Decreased lung tissue burden of Δ*cnaA* mutant infection

A. fumigatus strain	Log_{10} CFU/g lung tissue (mean ± SE) at:		
	Day +3 of infection	Day +5 of infection	Day +7 of infection
Wild type	3.96 ± 0.04[a]	4.28 ± 0.09[a]	4.26 ± 0.06[a]
Δ*cnaA* mutant	2.88 ± 0.11	2.87 ± 0.17	2.83 ± 0.12
Δ*cnaA* + *cnaA*	4.19 ± 0.08[a]	3.86 ± 0.11[b]	4.47 ± 0.08[a]

[a] $P < 0.001$ versus result for the Δ*cnaA* mutant.
[b] $P = 0.001$ versus result for the Δ*cnaA* mutant.

Similarly to all other infectious pathogens, *Aspergillus* growth plays a crucial role in the establishment of human disease. This is underscored by the fact that the two most effective classes of antifungals for the preferred treatment of invasive aspergillosis both inhibit growth of *A. fumigatus* as their mechanism of action. The triazole class of antifungals inhibits ergosterol production in the fungal cell membrane, while the echinocandin class inhibits glucan synthesis in the fungal cell wall. In one study there was a direct correlation between in vitro growth and in vivo virulence of *A. fumigatus* in an animal model (26), indicating that genes involved in growth of the fungus are likely important pathogenicity determinants as invasive disease is established. For instance, disruption of *A. fumigatus rasB*, a gene involved in morphogenesis (12), *cgrA*, a gene suspected to be involved in ribosome synthesis (4), or *rhbA*, a gene implicated in nitrogen sensing (27), showed defects in growth and attenuated disease in an animal model. However, disruption of each of these genes did not yield the same severity of growth interruption or pathogenicity attenuation as the Δ*cnaA* mutant.

Hyphal growth in *A. fumigatus* appears to occur through apical extension from a germling, but the molecular mechanisms underlying this extension and their contributions to virulence are unknown. In a concurrent work utilizing a Ku80 mutant background of *A. fumigatus* (10a), there is brief mention of a growth defect in a mutant lacking calcineurin A (referred to as *calA*) but no report on virulence. Our results actually suggest that calcineurin controls key steps in hyphal polarized growth and morphology in *A. fumigatus* hyphae and the critically important ability to invade tissue with this growth. Our Δ*cnaA* mutant can form septations but is profoundly limited in its apical extension. Our previous work with pharmacologic calcineurin inhibitors suggested a role for calcineurin in hyphal extension and an impact on the fungal cell wall since our Δ*cnaA* mutant phenotype was similar to that of *A. fumigatus* treated with an echinocandin antifungal which specifically targets the β-(1, 3)-D-glucan synthase (36). Preliminary staining with the cell viability fluorescent dyes 5,(6)-carboxyfluorescein diacetate (CFDA) and bis-(1,3-dibutylbarbituric acid) trimethine oxonol (DiBAC), which stain live and dead cells, respectively, also localized the antifungal activity of calcineurin inhibitors to the hyphal tips. Furthermore, the hyphal morphology of the Δ*cnaA* mutant is similar to the growth arrest and increase in hyphal branching seen with inducible expression of antisense RNA of calcineurin A in the nonpathogenic model filamentous fungus *Neurospora crassa* (29). Similarly, RNA interference silencing of calcineurin B in the model slime mold *Dictyostelium discoideum* resulted in cells with short stalks and spore heads with additional tips (6), a phenotype likely related to that observed with the *A. fumigatus* Δ*cnaA* mutant. In contrast, calcineurin plays little or no demonstrable role in filamentous growth in the invasive dimorphic fungal pathogen *C. albicans* (3, 5), highlighting that the role of this conserved gene differs among opportunistic fungal pathogens.

Few genetic mutants of *A. fumigatus* created so far have led to defects in survival when tested in animal models. Furthermore, most other *A. fumigatus* mutants created to date have been tested for pathogenicity defects only in that laboratory's single animal model. With the potential inherent differences in each laboratory's model system and the lack of effective standardizations, it may be difficult to compare interlaboratory results and make definitive statements on the virulence of mutants. Therefore, we purposefully tested our Δ*cnaA* mutant in five fundamentally distinct animal models at two independent laboratories to conclusively confirm the profound defect in pathogenicity of the Δ*cnaA* mutant. The power of this approach is the specific differences in each animal model all pointing toward the same conclusion of the lack of virulence of the Δ*cnaA* mutant.

Multiple animal models of invasive aspergillosis were used to assess questions of both the effect of host immune function on the Δ*cnaA* mutant and disease progression, as well as the in vitro conidial and hyphal defects of the Δ*cnaA* mutant and in vivo disease establishment. The wide spectrum of animal models used helped answer both important questions. The animals' immune function status included profoundly and persistently immunosuppressed animals with repeated doses of two mechanistically different agents in both inhalational models, transiently immunosuppressed animals with a single dose of a single agent in the intranasal model, a fully immunocompetent animal in the intravenous model, and an immunocompetent invertebrate animal, which possesses a remarkably simpler immune system, in the wax moth model.

The invertebrate wax moth model has been used recently to gauge *A. fumigatus* virulence (17, 31), and this unique newer model again revealed a difference in the Δ*cnaA* mutant versus the wild-type and Δ*cnaA* + *cnaA* strains. Here the growth of the Δ*cnaA* mutant was severely restricted in an environment without high temperatures and without the demands of a sophisticated innate and adaptive immunity as seen in the mammalian models. This crucial difference helps to separate the organism's ability to grow in the host, which proves more difficult in the complex mammalian system with its changing immunity and immunosuppression. Clearly the immunosuppressed mammalian models are useful and clinically relevant, but they are also systems where we and others have demonstrated the importance of the host immune system playing a vital and complex role in the establishment and outcome of infection (35). In the more complex models, it is increasingly more difficult to separate organism damage from host damage. However, with the addition of this simpler moth model to more completely explore various host immunologic backgrounds, we appreciate the direct impact of severely restricted fungal growth on the pathogenesis and outcome of invasive disease.

The issues of infectious delivery and its role in the lack of pathogenicity of the Δ*cnaA* mutant were equally evaluated in the multiple animal models. Since the Δ*cnaA* mutant possessed a conidial defect, it was important to validate that this defect alone did not affect pathogenicity. While examination of CFU in the lungs after 1 h of infection in the inhalational models demonstrated that there were significant differences in the conidia reaching the alveoli, it was conceivable that a mutant with a defect which created large chains of conidia might bias an aerosol model which required inhalation of the organism. Therefore, we also utilized an intranasal model (12) with direct instillation in the animal's nares to circumvent any unknown aerosolization issues that a conidial defect might confer.

As a final validation that inoculum delivery methodology was not the sole reason for a profound difference in pathogenicity, an intravenous inoculation was utilized to definitively nullify any conidial defect that might affect delivery of the fungus to the tissue. Here the conidia were directly intravenously injected into the animal. While this model does not, in our opinion, accurately mimic human acquisition of invasive aspergillosis, the system has been utilized successfully in the past to adequately create invasive disease. For our purposes, the direct injection allowed elimination of all experimental variables related to initial delivery of inoculum and still demonstrated the substantial effect of the Δ*cnaA* mutant on growth in the host tissue.

Taken together, our results provide evidence that calcineurin is profoundly involved in *A. fumigatus* growth, infectivity, tissue invasion, and finally pathogenicity. Calcineurin is an excellent therapeutic target that could potentially be used to improve outcomes of IA, as it centers on halting the otherwise robust growth of this fungus. The best predictor of a patient's likelihood of survival from IA is recovery of immune function, as the current antifungal armamentarium largely serves only to delay growth and progression of this deadly fungus until the body mounts an effective immune response. Drastically slowing

the proliferation of *A. fumigatus* allows time for immune system recovery and direct antifungal drug effects, thus substantially improving outcome by reducing tissue destruction. This paradigm has been validated by the success of the echinocandin beta-glucan synthase inhibitors in the treatment of invasive aspergillosis (20). Since the Δ*cnaA* mutation stunts growth of *A. fumigatus* in multiple in vitro formats, resulting in a lack of hyphal invasion in the infected lung and a dramatic attenuation of pathogenicity in multiple distinct animal models, this target should also have great potential as an antifungal strategy for newer agents.

Improving patient survival with IA remains a challenge, and harnessing the conserved calcineurin pathway offers considerable promise. Our studies reveal that calcineurin plays a conserved role in fungal pathobiology but via unique specialization across the different fungal genera and now even *Aspergillus* species. The shared role of calcineurin in mediating fungal growth in vitro and in vivo and subsequent inability to establish invasive disease may be exploitable with drug analogs that target this fungal Achilles' heel yet spare host calcineurin function. As demonstrated in other disease processes where this pathway can be modulated to improve outcomes (1, 28, 38), our data suggest that this may be possible for IA. The exciting prospect lies in modulating in vivo fungal growth to drastically stunt the growth, invasiveness, and ultimately mortality of IA.

ACKNOWLEDGMENTS

We thank Leslie Eibest for assistance with the scanning electron microscopy images, Alexander Indrum for assistance with the wax moth model, Andrew Alspaugh for assistance with technical aspects of the study, and John R. Graybill for assistance with the second inhalational animal model.

This work was supported by National Institutes of Health grant 1 K08 A1061149 and a Children's Oncology Group Young Investigator award to W.J.S., a National Institutes of Health training grant to R.A.C., an NSF award for the scanning electron microscopy to Leslie Eibest, and a National Institutes of Health contract to T.F.P. for the second inhalational animal model.

REFERENCES

1. **Alexander, A. G., N. C. Barnes, and A. B. Kay.** 1992. Trial of cyclosporin in corticosteroid-dependent chronic severe asthma. Lancet **339:**324–328.
2. **Aperia, A., F. Ibarra, L.-B. Svensson, C. B. Klee, and P. Greengard.** 1992. Calcineurin mediates alpha-adrenergic stimulation of Na+, K+-ATPase activity in renal tubule cells. Proc. Natl. Acad. Sci. USA **89:**7394–7397.
3. **Bader, T., B. Bodendorfer, K. Schroppel, and J. Morschhauser.** 2003. Calcineurin is essential for virulence in *Candida albicans*. Infect. Immun. **71:** 5344–5354.
4. **Bhabhra, R., M. D. Miley, E. Mylonakis, D. Boettner, J. Fortwendel, J. C. Panepinto, M. Postow, J. C. Rhodes, and D. S. Askew.** 2004. Disruption of the *Aspergillus fumigatus* gene encoding nucleolar protein CgrA impairs thermotolerant growth and reduces virulence. Infect. Immun. **72:**4731–4740.
5. **Blankenship, J. R., F. L. Wormley, M. K. Boyce, W. A. Schell, S. G. Filler, J. R. Perfect, and J. Heitman.** 2003. Calcineurin is essential for *Candida albicans* survival in serum and virulence. Eukaryot. Cell **2:**422–430.
6. **Boeckeler, K., G. Tischendorf, R. Mutzel, and B. Weissenmayer.** 2006. Aberrant stalk development and breakdown of tip dominance in Dictyostelium cell lines with RNAi-silenced expression of calcineurin B. BMC Dev. Biol. **6:**12–22.
7. **Bok, J. W., and N. P. Keller.** 2004. LaeA, a regulator of secondary metabolism in *Aspergillus* spp. Eukaryot. Cell **3:**527–535.
8. **Capilla Luque, J., K. V. Clemons, and D. A. Stevens.** 2003. Efficacy of micafungin alone or in combination against systemic murine aspergillosis. Antimicrob. Agents Chemother. **47:**1452–1455.
9. **Clipstone, N. A., and G. R. Crabtree.** 1992. Identification of calcineurin as a key signalling enzyme in T-lymphocyte activation. Nature **357:**695–697.
10. **Cruz, M. C., D. S. Fox, and J. Heitman.** 2001. Calcineurin is required for hyphal elongation during mating and haploid fruiting in Cryptococcus neoformans. EMBO J. **20:**1020–1032.
10a. **da Silva Ferreira, M. E., M. R. V. Z. Kress, M. Savoldi, M. H. S. Goldman, A. Härtl, T. Heinekamp, A. A. Brakhage, and G. H. Goldman.** 2006. The *akuB*^{KU80} mutant deficient for nonhomologous end joining is a powerful tool for analyzing pathogenicity in *Aspergillus fumigatus*. Eukaryot. Cell **5:**207–211.
11. **Ferreira, A., R. Kincaid, and K. S. Kosik.** 1993. Calcineurin is associated with the cytoskeleton of cultured neurons and has a role in the acquisition of polarity. Mol. Biol. Cell **4:**1225–1238.
12. **Fortwendel, J. R., W. Zhao, R. Bhabhra, S. Park, D. S. Perlin, D. S. Askew, and J. C. Rhodes.** 2005. A fungus-specific Ras homolog contributes to the hyphal growth and virulence of *Aspergillus fumigatus*. Eukaryot. Cell **4:**1982–1989.
13. **Fox, D. S., M. C. Cruz, R. A. L. Sia, H. Ke, G. M. Cox, M. E. Cardenas, and J. Heitman.** 2001. Calcineurin regulatory subunit is essential for virulence and mediates interactions with FKBP12-FK506 in Cryptococcus neoformans. Mol. Microbiol. **39:**835–849.
14. **Galagan, J. E., S. E. Calvo, C. Cuomo, L. J. Ma, J. R. Wortman, S. Batzoglou, S. I. Lee, M. Basturkmen, C. C. Spevak, J. Clutterbuck, V. Kapitonov, J. Jurka, C. Scazzocchio, M. Farman, J. Butler, S. Purcell, S. Harris, G. H. Braus, O. Draht, S. Busch, C. D'Enfert, C. Bouchier, G. H. Goldman, D. Bell-Pedersen, S. Griffiths-Jones, J. H. Doonan, J. Yu, K. Vienken, A. Pain, M. Freitag, E. U. Selker, D. B. Archer, M. A. Penalva, B. R. Oakley, M. Momany, T. Tanaka, T. Kumagai, K. Asai, M. Machida, W. C. Nierman, D. W. Denning, M. Caddick, M. Hynes, M. Paoletti, R. Fischer, B. Miller, P. Dyer, M. S. Sachs, S. A. Osmani, and B. W. Birren.** 2005. Sequencing of *Aspergillus nidulans* and comparative analysis with *A. fumigatus* and *A. oryzae*. Nature **438:**1105–1115.
15. **Groll, A. H., P. M. Shah, C. Mentzel, M. Schneider, G. Just-Neubling, and K. Heubner.** 1996. Trends in the postmortem epidemiology of invasive fungal infections at a university hospital. J. Infect. **33:**23–32.
16. **Kidd, S. E., F. Hagen, R. L. Tscharke, M. Huynh, K. H. Bartlett, M. Fyfe, L. Macdougall, T. Boekhout, K. J. Kwon-Chung, and W. Meyer.** 2004. A rare genotype of Cryptococcus gattii caused the cryptococcosis outbreak on Vancouver Island (British Columbia, Canada). Proc. Natl. Acad. Sci. USA **101:** 17258–17263.
17. **Krappmann, S., C. Sasse, and G. H. Braus.** 2006. Gene targeting in *Aspergillus fumigatus* by homologous recombination is facilitated in a nonhomologous end-joining-deficient genetic background. Eukaryot. Cell **5:**212–215.
18. **Liu, F., I. Grundke-Iqbal, K. Iqbal, Y. Oda, K. Tomizawa, and C. X. Gong.** 2005. Truncation and activation of calcineurin A by calpain I in Alzheimer disease brain. J. Biol. Chem. **280:**37755–37762.
19. **Liu, J., J. D. Farmer, Jr., W. S. Lane, J. Friedman, I. Weissman, and S. L. Schreiber.** 1991. Calcineurin is a common target of cyclophilin-cyclosporin A and FKBP-FK506 complexes. Cell **66:**807–815.
20. **Maertens, J., I. Raad, G. Petrikkos, M. Boogaerts, D. Selleslag, F. B. Petersen, C. A. Sable, N. A. Kartsonis, A. Ngai, A. Taylor, T. F. Patterson, D. W. Denning, and T. J. Walsh.** 2004. Efficacy and safety of caspofungin for treatment of invasive aspergillosis in patients refractory to or intolerant of conventional antifungal therapy. Clin. Infect. Dis. **39:**1563–1571.
21. **Marr, K. A., R. A. Carter, F. Crippa, A. Wald, and L. Corey.** 2002. Epidemiology and outcome of mould infections in hematopoietic stem cell transplant recipients. Clin. Infect. Dis. **34:**909–917.
22. **McNeil, M. M., S. L. Nash, R. A. Hajjeh, M. A. Phelan, L. A. Conn, B. D. Plikaytis, and D. W. Warnock.** 2001. Trends in mortality due to invasive mycotic diseases in the United States, 1980–1997. Clin. Infect. Dis. **33:**641–647.
23. **Mylonakis, E., R. Moreno, J. B. El Khoury, A. Indrum, J. Heitman, S. B. Calderwood, F. M. Ausubel, and A. Diener.** 2005. *Galleria mellonella* as a model system to study *Cryptococcus neoformans* pathogenesis. Infect. Immun. **73:**3842–3850.
24. **Odom, A., S. Muir, E. Lim, D. L. Toffaletti, J. R. Perfect, and J. Heitman.** 1997. Calcineurin is required for virulence of Cryptococcus neoformans. EMBO J. **16:**2576–2589.
25. **Osherov, N., D. P. Kontoyiannis, A. Romans, and G. S. May.** 2001. Resistance to itraconazole in *Aspergillus nidulans* and *Aspergillus fumigatus* is conferred by extra copies of the *A. nidulans* P-450 14alpha-demethylase gene, pdmA. J. Antimicrob. Chemother. **48:**75–81.
26. **Paisley, D., G. D. Robson, and D. W. Denning.** 2005. Correlation between in vitro growth rate and in vivo virulence in Aspergillus fumigatus. Med. Mycol. **43:**397–401.
27. **Panepinto, J. C., B. G. Oliver, J. R. Fortwendel, D. L. Smith, D. S. Askew, and J. C. Rhodes.** 2003. Deletion of the *Aspergillus fumigatus* gene encoding the Ras-related protein RhbA reduces virulence in a model of invasive pulmonary aspergillosis. Infect. Immun. **71:**2819–2826.
28. **Ponticelli, C., and P. Passerini.** 2001. Alternative treatments for focal and segmental glomerulosclerosis. Clin. Nephrol. **55:**345–348.
29. **Prokisch, H., O. Yarden, M. Dieminger, M. Tropschug, and I. B. Barthelmess.** 1997. Impairment of calcineurin function in Neurospora crassa reveals its essential role in hyphal growth, morphology and maintenance of the apical Ca2+ gradient. Mol. Gen. Genet. **256:**101–114.
30. **Rasmussen, C., C. Garen, S. Brining, R. L. Kincaid, R. L. Means, and A. R. Means.** 1994. The calmodulin-dependent protein phosphatase catalytic subunit (calcineurin A) is an essential gene in Aspergillus nidulans. EMBO J. **13:**2545–2552.
31. **Reeves, E. P., C. G. M. Messina, and K. Kavanagh.** 2004. Correlation between gliotoxin production and virulence of *Aspergillus fumigatus* in *Galleria mellonella*. Mycopathologia **158:**73–79.

32. **Reiken, S., X. H. T. Wehrens, J. A. Vest, A. Barbone, S. Klotz, D. Mancini, D. Burkhoff, and A. R. Marks.** 2003. Beta-blockers restore calcium release channel function and improve cardiac muscle performance in human heart failure. Circulation **107:**2459–2466.
33. **Sanglard, D., F. Ischer, O. Marchetti, J. Entenza, and J. Bille.** 2003. Calcineurin A of Candida albicans: involvement in antifungal tolerance, cell morphogenesis and virulence. Mol. Microbiol. **48:**959–976.
34. **Shimizu, K., and N. P. Keller.** 2001. Genetic involvement of a cAMP-dependent protein kinase in a G protein signaling pathway regulating morphological and chemical transitions in Aspergillus nidulans. Genetics **157:**591–600.
35. **Steinbach, W. J., D. K. J. Benjamin, S. A. Trasti, J. L. Miller, W. A. Schell, A. K. Zaas, W. M. Foster, and J. R. Perfect.** 2004. Value of an inhalational model of invasive aspergillosis. Med. Mycol. **42:**417–425.
36. **Steinbach, W. J., W. A. Schell, J. R. Blankenship, C. Onyewu, J. Heitman, and J. R. Perfect.** 2004. In vitro interactions between antifungals and immunosuppressants against *Aspergillus fumigatus*. Antimicrob. Agents Chemother. **48:**1664–1669.
37. **Storb, R., H. J. Deeg, J. Whitehead, F. Appelbaum, P. Beatty, W. Bensinger, C. D. Buckner, R. Clift, K. Doney, and V. Farewell.** 1986. Methotrexate and cyclosporine compared with cyclosporine alone for prophylaxis of acute graft versus host disease after marrow transplantation for leukemia. N. Engl. J. Med. **314:**729–735.
38. **Temekonidis, T. I., A. N. Georgiadis, Y. Alamanos, D. V. Bougias, P. V. Voulgari, and A. A. Drosos.** 2002. Infliximab treatment in combination with cyclosporin A in patients with severe refractory rheumatoid arthritis. Ann. Rheum. Dis. **61:**822–825.
39. **Thau, N., M. Monod, B. Crestani, C. Rolland, G. Tronchin, J.-P. Latgé, and S. Paris.** 1994. *rodletless* mutants of *Aspergillus fumigatus*. Infect. Immun. **62:**4380–4388.